JOURNAL OF CHEMICAL & ENGINEERING DATA

ARTICLE

pubs.acs.org/jced

Phase Equilibria in Binary Mixtures of Propane and Phenanthrene: Experimental Data and Modeling with the GC-EoS

Bianca Breure,[†] Eugene J. M. Straver,[‡] Louw J. Florusse,[‡] Marijn P. W. M. Rijkers,[‡] Ioannis G. Economou,[†] Francisco M. Vargas,[†] and Cor J. Peters*[,†,‡]

[†]The Petroleum Institute Department of Chemical Engineering P.O. Box 2533, Abu Dhabi, United Arab Emirates

[‡]Delft University of Technology Faculty of Mechanical, Maritime and Materials Engineering Department of Process and Energy Leeghwaterstraat 44, 2622 CA Delft, The Netherlands

ABSTRACT: In this paper experimental data are presented for the binary system propane + phenanthrene. Experimental measurements have been performed for various two-phase and three-phase equilibria, including equilibria in the presence of solid phenanthrene. Based on the course of the various three-phase equilibria, an estimation could be made for the location of the quadruple point solid phenanthrene-liquid−liquid−vapor (SL_1L_2G). Experimental work was performed for the temperature range $337 < T/K < 434$ and pressures up to 22 MPa. Besides phase equilibrium data also liquid phenanthrene volume measurements are presented for temperatures between (377 and 425) K and pressure varying between (2 and 10) MPa. The experimental phase behavior data were compared to predictions made with the group contribution equation of state, resulting generally in a good agreement.

INTRODUCTION

Supercritical fluid extraction has proven to be a very useful and reliable separation technology for the chemical, petrochemical, and pharmaceutical industry. Besides the widely used extractants carbon dioxide and ethylene, also propane might be a suitable candidate as solvent for supercritical fluid applications.

In order to develop processes for the extraction of poly aromatic compounds, such as naphthalene, acenaphthene and phenanthrene, with propane reliable phase equilibrium data are required to determine optimal regions for operation. If, in addition, the phase behavior of these aliphatic-poly aromatic systems can be described accurately by an equation of state, design of the extraction process and its optimization can be greatly simplified. Furthermore, studying systems of hydrocarbons and poly aromatics may contribute to a better understanding of the phase behavior of complex mixtures, such as crude oils and the development of appropriate thermodynamic models to describe their phase behavior, including phenomena such as asphaltene precipitation.

Systems consisting of a volatile solvent composed of small molecules, such as propane, and a solute consisting of low volatile, complex molecules, such as poly aromatic compounds, are known to show complex phase behavior.[1] Multiphase fluid behavior can occur and also a solid phase may be present, which further increases the complexity of the phase diagrams.

This paper presents experimental results on the phase behavior of binary mixtures of propane with phenanthrene. This binary system is known to show type-III fluid phase behavior according to the classification of Van Konynenburg and Scott.[3] Both two-phase and three-phase equilibria are studied, including phase equilibria with a solid phenanthrene phase. The experimental data are compared to predictions with the Group Contribution Equation of State (GC-EoS).

THEORY

As stated in earlier work,[1,2] the binary system propane + phenanthrene shows type III behavior in the classification of Van Konynenburg and Scott.[3] This type of phase behavior is characterized by the presence of a three-phase L_1L_2G equilibrium, which ends in a critical end point of the type $L_1 = G + L_2$ (also called K point). This critical end point is connected to the critical end point of the more volatile component through the critical locus $L_1 = G$. Another branch of the critical locus originates in the critical point of the less volatile component and extends to lower temperatures and higher pressures, while changing its nature from $L_2 = G$ to $L_1 = L_2$. This curve characteristically shows a pressure minimum.

The phase behavior of fluid systems becomes more complicated in the presence of a solid phase. The p,T diagram may then contain a nonvariant quadruple point (Q-point) SL_1L_2G as a result of the intersection of the two three-phase equilibria L_1L_2G and SLG. From the quadruple point four three-phase equilibria originate, namely SL_1G, SL_2G, SL_1L_2 and L_1L_2G. This type of phase behavior is also observed for the propane + phenanthrene system, as a result of the formation of a solid phase by the nonvolatile component phenanthrene. Figure 1 shows a typical p,T diagram for type III fluid phase behavior in the presence of a solid phase.

EXPERIMENTAL SECTION

The experimental work was carried out in a so-called Cailletet apparatus, which has been described extensively in literature. For details on the apparatus and the experimental procedures one is referred to refs 4−6.

Special Issue: John M. Prausnitz Festschrift

Received: October 30, 2010
Accepted: March 2, 2011
Published: March 18, 2011

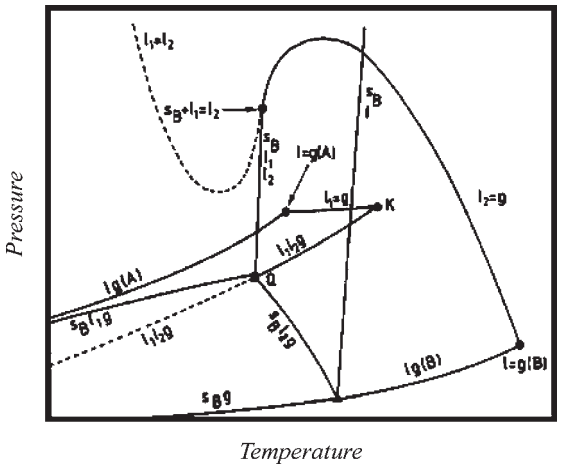

Figure 1. Type III of fluid phase behavior in the classification of Scott and Van Konynenburg[3] in the presence of a solid solute phase (B).

Phenanthrene was available with a purity of 0.99 mol fraction and was further purified by zone-melting until a homogeneous brownish-orange color was obtained. The main contaminant in phenanthrene was anthracene, an isomer with a considerably higher melting point than phenanthrene (492.65 K versus 372.35 K). Propane was available at a purity of 0.9991 mol fraction. The inaccuracy of the experiments was as follows: pressure 0.002 MPa over the whole pressure range; temperature 0.01 K; composition 0.001 in the mole fraction; volumetric measurements 0.002 $cm^3 \cdot mol^{-1}$. All experimental data were the average of at least duplicate measurements.

THERMODYNAMIC MODELING

The GC-EoS developed by Skjold-Jørgensen[7,8] is an equation of state expressed in terms of the residual Helmholtz energy, which is taken as the sum of an attractive term and a free volume contribution. The attractive term is a group contribution version of a density-dependent NRTL-type expression, whereas the free volume term is based on the Carnahan−Starling equation for hard spheres. The equations that form the basis for the GC-EoS are extensively described in literature and will not be repeated here. For more details about the GC-EoS and its constituting equations one is referred to refs 7−9.

The free volume term requires a value for the critical hard sphere diameter ($d_{C,i}$/cm·mol^{-1}) of the pure components, which can be calculated from their critical properties according to

$$d_{C,i} = \left(\frac{0.08943 R T_{C,i}}{P_{C,i}}\right)^{1/3} \quad (1)$$

where R/atm·cm^3·mol^{-1}·K^{-1} is the universal gas constant, $T_{C,i}$/K the critical temperature, and $P_{C,i}$/atm the critical pressure. Values for the critical properties for phenanthrene are reported in ref 10. Fornari[9] published a comprehensive overview of the GC-EoS including parameter tables containing pure group, binary interaction, and binary nonrandomness parameters for various groups to be used in the attractive contribution of the residual Helmholtz energy.

In order to model the propane + phenanthrene system, it was decided to regard phenanthrene as a single group. Decomposition of phenanthrene into aromatic CH_2 and CH groups did not result in satisfactory results. For example, the deviation between experimental and calculated bubble point data is very large when phenanthrene is decomposed in subgroups, as is illustrated in Figure 2. The average absolute relative deviation for the different data sets varied between 20.2 % and 38.7 %.

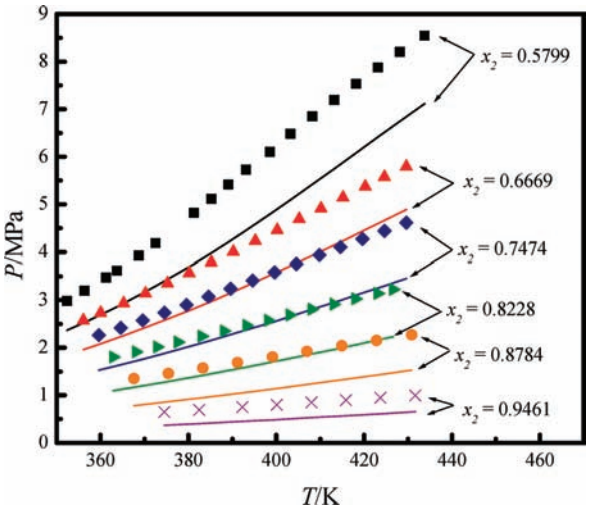

Figure 2. Comparison between experimental and calculated bubble point data for the system propane + phenanthrene. Propane is decomposed into two CH_3 and one CH_2 group and phenanthrene into ten ACH groups and four AC groups. Simulations are run with data taken from ref 9.

Propane was decomposed in a single CH_2-group and two CH_3 groups, for which parameters could be found in the tables published by Fornari.[9] Because phenanthrene was regarded as a new single group, values for the pure group parameters T^*/K, q, g^*/cm^6·atm·mol^{-2}, and g' had to be determined (g'' was taken to be zero) as well as interaction (k_{ij}^* and k_{ij}') and nonrandomness parameters (a_{ij} and a_{ji}) between the two alkyl groups and phenanthrene. The value for the van der Waals molecular surface area q was determined by taking the sum of the UNIFAC group area parameters ACH and AC, which are reported in ref 10. The reference temperature was set equal to the critical temperature of phenanthrene (T^* = 869 K[10]). The pure group parameters g^*,g' were determined by fitting phenanthrene vapor pressure data taken from ref 11, the DIPPR database and ref 12. The binary interaction and nonrandomness parameter were fitted to bubble point data of the propane + phenanthrene system at phenanthrene mole fractions of $0.5799 \le x \le 0.9461$ (see Table 2). For each mole fraction only the data for the lowest and highest temperature were used in the fitting process. In order to determine the binary parameters it was assumed that phenanthrene interacts in a similar way with the CH_3 group as with the CH_2 group and hence $k^*_{CH_3\text{-phen}} = k^*_{CH_2\text{-phen}}$, $k'_{CH_3\text{-phen}} = k'_{CH_2\text{-phen}}$ and $\alpha_{CH_3\text{-phen}} = \alpha_{CH_2\text{-phen}}$. Furthermore, it was assumed that the nonrandomness parameters are symmetrical: $\alpha_{CH_3\text{-phen}} = \alpha_{phen\text{-}CH_3}$ and $\alpha_{CH_2\text{-phen}} = \alpha_{phen\text{-}CH_2}$. The values of the pure group parameters and binary interaction parameters and nonrandomness parameters that are used in this work are shown in Table 1.

As mentioned, the GC-EoS is an equation of state in terms of the residual Helmholtz energy. By adding an expression for the ideal gas Helmholtz energy to the residual term, an expression for the Helmholtz energy can be obtained. Latter expression can be used to derive expressions for the fugacity coefficients that are required in phase equilibrium calculations. Because equations of state are limited to describe fluid phases, another approach is

Table 1. Pure Group Parameters, Binary Interaction Parameters, and Nonrandomness Parameters Used in This Work

Pure Group Parameters					
group	T^*/K	q	g^{*a}	g'	g''
CH_3	600	0.848	316910.0	−0.9274	0
CH_2	600	0.540	356090.0	−0.8755	0
phenanthrene	869	4.48	893467.1	−0.8495	0

Binary Interaction Parameters and Nonrandomness Parameters					
i	j	k_{ij}^*	k'_{ij}	α_{ij}	α_{ji}
phenanthrene	CH_3	0.9753	-1.783×10^{-5}	−0.5083	−0.5083
phenanthrene	CH_2	0.9753	-1.783×10^{-5}	−0.5083	−0.5083
CH_3	CH_2	1	0	0	0

[a] In cm^6 atm mol^{-2}.

used to describe the solid phase. Furthermore, phenanthrene shows a transition between two crystal structures in the solid phase (a so-called lambda point transition) and this effect should be accounted for as it can affect its solubility.[13] The fugacity of the pure solid phase (f^{solid}/kPa) is related to the fugacity of the pure subcooled liquid ($f^{sub.liq}$/kPa) according to the procedure described by ref 13

$$\Delta g_{sub.liq\text{-}solid} = RT_{sys} \ln\left(\frac{f^{sub.liq}}{f^{solid}}\right) \quad (2)$$

$$\ln\left(\frac{f^{sub.liq}}{f^{solid}}\right) = \frac{1}{RT_{sys}}\int_{T=T_{sys}}^{T=T_t} c_p^{solid}\left(1-\frac{T_{sys}}{T}\right) dT - \frac{1}{RT_{sys}}\int_{T=T_{sys}}^{T=T_t} c_p^{liquid}\left(1-\frac{T_{sys}}{T}\right) dT + \frac{\Delta h_{fus}}{RT_{sys}}\left(1-\frac{T_{sys}}{T_t}\right) \quad (3)$$

where R/kJ·kmol^{-1}·K^{-1} is the universal gas constant, T_{sys}/K the temperature of the system, T_t/K is the triple point temperature of phenanthrene, c_p^{solid}/kJ·kmol^{-1}·K^{-1} the heat capacity of solid phenanthrene, c_p^{liquid}/kJ·kmol^{-1}·K^{-1} the heat capacity of liquid phenanthrene, and Δh_{fus}/kJ·kmol^{-1}the heat of fusion. Data for the heat capacities of phenanthrene in the liquid and solid phases (including heat capacities during the lambda point transition) as a function of temperature were taken from ref 14. They also reported a value of $16.474 \cdot 10^3$ kJ·kmol^{-1} for the heat of fusion of phenanthrene at the triple point of 372.4 K. All multiphase equilibrium calculations were performed in Matlab using the numerical procedure described by ref 15. In order to solve the integrals in eq 3 the heat capacities were correlated to temperature using piecewise cubic Hermite splines.

EXPERIMENTAL RESULTS

Table 2 shows experimental data on the L_1L_2 miscibility, bubble point, and melting point lines of the propane + phenanthrene system. Three phase measurements are summarized in Table 3. Four different three-phase lines were measured directly, namely for SL_2G, L_1L_2G, SL_1G, and SL_1L_2 three phase equilibria. The presence of four three-phase equilibria indicates the presence of a SL_1L_2G quadruple point. The L_1L_2G three phase line starts at the quadruple point and terminates at the Upper Critical End Point L_1L_2 = G which is included in Table 3. The SL_1L_2

Table 2. Immiscibility, Bubble, and Melting Points for the Propane (1) + Phenanthrene (2) System for Various Values of the Phenanthrene Mole Fraction x_2

T/K	p/MPa	T/K	p/MPa	T/K	p/MPa
		$L_1(L_2)$ Lines ($x_2 = 0.0294$)			
350.68	2.885	366.42	4.622	399.31	8.260
354.58	3.110	371.41	5.132	405.32	8.795
354.66	3.358	376.38	5.8360	411.34	9.269
357.72	3.330	381.39	6.3910	417.35	9.644
359.58	3.897	387.37	7.0340		
363.53	4.381	393.33	7.6740		
		$L_1(L_2)$ Lines ($x_2 = 0.0396$)			
356.02	5.596	385.87	8.044	415.83	10.499
361.98	5.957	391.86	8.509	421.80	10.909
367.96	6.449	397.85	9.047	427.75	11.292
373.92	7.054	403.82	9.564		
379.91	7.549	409.83	10.054		
		$L_1(L_2)$ Lines ($x_2 = 0.0494$)			
351.82	7.709	361.63	7.850	384.34	9.130
351.94	7.730	361.71	7.809	392.22	9.690
354.32	7.740	364.16	7.980	400.06	10.240
356.75	7.720	366.66	8.070	407.90	10.790
356.81	7.749	371.56	8.340	415.75	11.360
359.18	7.780	376.49	8.650	423.60	11.850
		$L_1(L_2)$ Lines ($x_2 = 0.0711$)			
353.52	12.665	371.19	11.865	390.26	12.255
362.54	12.085	381.11	11.965		
		$L_1(L_2)$ Lines ($x_2 = 0.1488$)			
353.62	20.955	381.01	16.750	407.83	16.185
362.89	18.885	390.16	16.310	417.56	16.290
372.09	17.5400	399.49	16.150		
		$L_2(L_1)$ Lines ($x_2 = 0.2499$)			
353.27	21.770	380.31	17.050	407.37	16.220
362.39	19.525	388.55	16.545	416.24	16.355
371.59	17.985	397.67	16.260	425.54	16.610
		$L_2(L_1)$ Lines ($x_2 = 0.3532$)			
353.77	19.930	381.56	15.550	408.64	14.970
363.04	17.815	389.76	15.110	418.17	15.160
372.39	16.410	399.38	14.930	427.42	15.480
		$L_2(L_1)$ Lines ($x_2 = 0.4529$)			
360.30	12.445	387.85	10.800	415.38	11.860
369.74	11.445	397.11	11.070	424.88	12.385
378.70	10.975	406.3	11.385		
		$L_2(L_1)$ Lines ($x_2 = 0.5394$)			
350.02	6.301	368.73	5.669	396.31	7.052
351.99	6.129	373.64	5.785	404.21	7.613
353.95	5.989	378.53	5.984	412.18	8.177
358.88	5.764	383.53	6.234	420.18	8.731
363.84	5.659	388.38	6.519	428.02	9.256
		$L_2(L_1)$ Lines ($x_2 = 0.5600$)			
351.21	4.151	375.93	4.756	412.32	7.574
356.20	4.047	380.87	5.141	420.01	8.107

dx.doi.org/10.1021/je101058b |J. Chem. Eng. Data 2011, 56, 1407–1413

Table 2. Continued

T/K	p/MPa	T/K	p/MPa	T/K	p/MPa
361.11	4.072	388.55	5.738	427.31	8.601
366.07	4.225	396.45	6.378		
370.99	4.440	404.33	6.991		
		L_2(G) Lines (x_2 = 0.5799)			
352.34	2.981	381.25	4.820	408.23	6.847
356.34	3.195	385.20	5.116	413.24	7.191
361.25	3.472	389.10	5.416	418.21	7.533
363.73	3.616	393.12	5.727	423.14	7.876
368.70	3.926	398.55	6.103	428.17	8.202
372.53	4.184	403.27	6.481	433.77	8.545
		L_2(G) Lines (x_2 = 0.6669)			
356.07	2.572	385.19	3.788	415.19	5.144
360.01	2.729	390.24	4.005	420.27	5.372
365.25	2.931	395.23	4.234	424.66	5.575
370.21	3.137	400.20	4.460	429.60	5.791
375.23	3.352	405.24	4.691		
380.18	3.569	410.17	4.915		
		L_2(G) Lines (x_2 = 0.7474)			
359.61	2.263	384.55	3.069	409.83	3.933
364.59	2.416	389.57	3.236	414.64	4.104
369.56	2.572	394.61	3.410	419.64	4.273
374.56	2.734	399.61	3.583	424.65	4.442
379.57	2.900	404.59	3.754	429.63	4.611
		L_2(G) Lines (x_2 = 0.8228)			
362.84	1.803	388.09	2.348	413.07	2.913
368.01	1.911	393.21	2.464	418.05	3.024
372.90	2.013	398.11	2.576	423.10	3.141
377.61	2.118	403.03	2.688	426.63	3.221
383.03	2.238	408.06	2.804		
		L_2(G) Lines (x_2 = 0.8784)			
367.60	1.353	391.20	1.687	414.93	2.037
375.46	1.461	399.12	1.803	422.81	2.153
383.32	1.572	406.99	1.920	430.81	2.270
		L_2(G) Lines (x_2 = 0.9461)			
374.51	0.647	400.12	0.801	423.67	0.950
382.42	0.694	407.99	0.851	431.65	0.997
392.25	0.753	415.84	0.900		
		L_1(S) Lines (x_2 = 0.0494)			
350.84	8.050	348.81	10.050	347.46	12.050
349.73	9.050	348.17	11.050		
		L_2(S) Lines (x_2 = 0.5394)			
351.43	7.050	351.85	9.050	352.33	11.050
351.63	8.050	352.07	10.050	352.56	12.050
		L_2(S) Lines (x_2 = 0.5600)			
351.40	4.550	352.15	7.550	352.88	10.551
351.77	6.050	352.53	9.050	353.26	12.051
		L_2(S) Lines (x_2 = 0.5799)			
351.54	3.251	352.21	6.051	352.80	8.551
351.82	4.552	352.59	7.551		

Table 2. Continued

T/K	p/MPa	T/K	p/MPa	T/K	p/MPa
		L_2(S) Lines (x_2 = 0.6669)			
355.68	3.051	356.30	5.051	357.41	9.051
356.02	4.051	356.80	7.051	358.00	11.052
		L_2(S) Lines (x_2 = 0.7474)			
358.43	3.047	359.04	5.047	360.25	9.048
358.74	4.047	359.64	7.047	360.83	11.048
		L_2(S) Lines (x_2 = 0.8228)			
362.93	3.051	363.55	5.050	364.81	9.050
363.22	4.051	364.19	7.050	365.45	11.051
		L_2(S) Lines (x_2 = 0.8784)			
365.95	1.951	367.43	6.552	368.81	11.052
366.43	3.551	367.83	8.051		
366.95	5.051	368.31	9.551		
		L_2(S) Lines (x_2 = 0.9461)			
370.29	1.051	371.31	4.051	372.32	7.051
370.79	2.551	371.82	5.551	372.89	8.550

Table 3. Three Phase Measurements for the Propane (1) + Phenanthrene (2) System

T/K	p/MPa	T/K	p/MPa	T/K	p/MPa
		SL_2G Line			
351.14	2.933	358.55	2.086	365.54	1.086
351.66	2.866	358.76	2.070	366.50	0.986
352.63	2.767	360.23	1.891	366.85	0.905
353.61	2.653	361.72	1.685	367.32	0.865
354.58	2.560	362.17	1.808	368.26	0.719
355.57	2.473	363.13	1.490	368.78	0.706
355.88	2.440	363.93	1.420	369.92	0.526
356.56	2.362	364.39	1.403	370.80	0.377
357.34	2.254	364.61	1.265		
357.54	2.238	365.42	1.184		
		L_1L_2G Line			
352.27	2.996	362.14	3.588	372.05	4.260
354.24	3.106	364.12	3.719	374.04	4.411
356.23	3.232	366.09	3.843	376.14	4.568
358.17	3.347	368.08	3.977	377.30	4.673
360.15	3.468	370.06	4.116	377.31	4.669*
*UCEP					
		SL_1G Line			
348.31	2.788	344.37	2.598	340.36	2.397
347.33	2.741	343.33	2.569	339.36	2.353
346.35	2.690	341.39	2.471	338.38	2.319
345.39	2.644	342.26	2.483	337.36	2.279
		SL_1L_2 Line			
351.09	3.307	351.16	3.943	351.09	5.751
351.27	3.521	351.02	4.931		

curve is expected to terminate in a $SL_1 = L_2$ critical point. From intersection of the four three-phase equilibria the location of the Q-point was estimated at 351.2 K and 2.928 MPa. Table 4 shows

Table 4. Liquid Phenanthrene Volume Measurements

T/K	p/MPa	v/cm^3·mol^{-1}	T/K	p/MPa	v/cm^3·mol^{-1}
377.69	2.049	167.865	385.54	2.049	168.811
	4.049	167.720		4.049	168.589
	6.049	167.416		6.049	168.269
	8.049	167.187		8.049	168.054
	10.049	167.042		10.049	167.932
393.38	2.049	169.845	401.26	2.049	170.765
	4.049	169.586		4.049	170.538
	6.049	169.222		6.049	170.173
	8.049	169.043		8.049	169.986
	10.049	168.925		10.049	169.812
409.13	2.049	171.738	417.06	2.049	172.777
	4.049	171.483		4.049	172.554
	6.049	171.219		6.049	172.255
	8.049	171.036		8.049	171.914
	10.049	170.903		10.049	171.750
424.84	2.049	173.794			
	4.049	173.544			
	6.049	173.229			
	8.049	172.902			
	10.049	172.734			

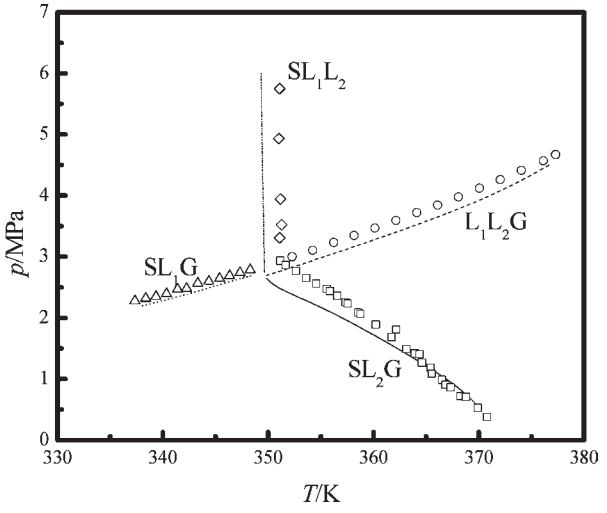

Figure 3. *p,T* diagram for the binary system propane-phenanthrene showing loci where three phases are in equilibrium. Comparison between predictions with the GC-EoS (lines) and experimental data (symbols).

results of liquid phenanthrene volume measurements for temperatures between (377 and 425) K and pressures up to 10 MPa.

Experimental Data versus Model Predictions. In Figure 3 a comparison is made between experimental data on the four three-phase equilibria SL_1G, SL_2G, L_1L_2G, and SL_1L_2, and predictions are done with the GC-EoS. The location of the quadruple point in the model predictions is shifted (to approximately 349.7 K and 2.7 MPa) compared to the experimental data and this also affects the paths of the curves SL_1L_2 and SL_2G. This deviation may be attributed to inaccuracies in the experimental solid phase heat capacities of phenanthrene and/or the temperature range over which the lambda point transition take place. According to data reported by ref 14, this lambda transition takes

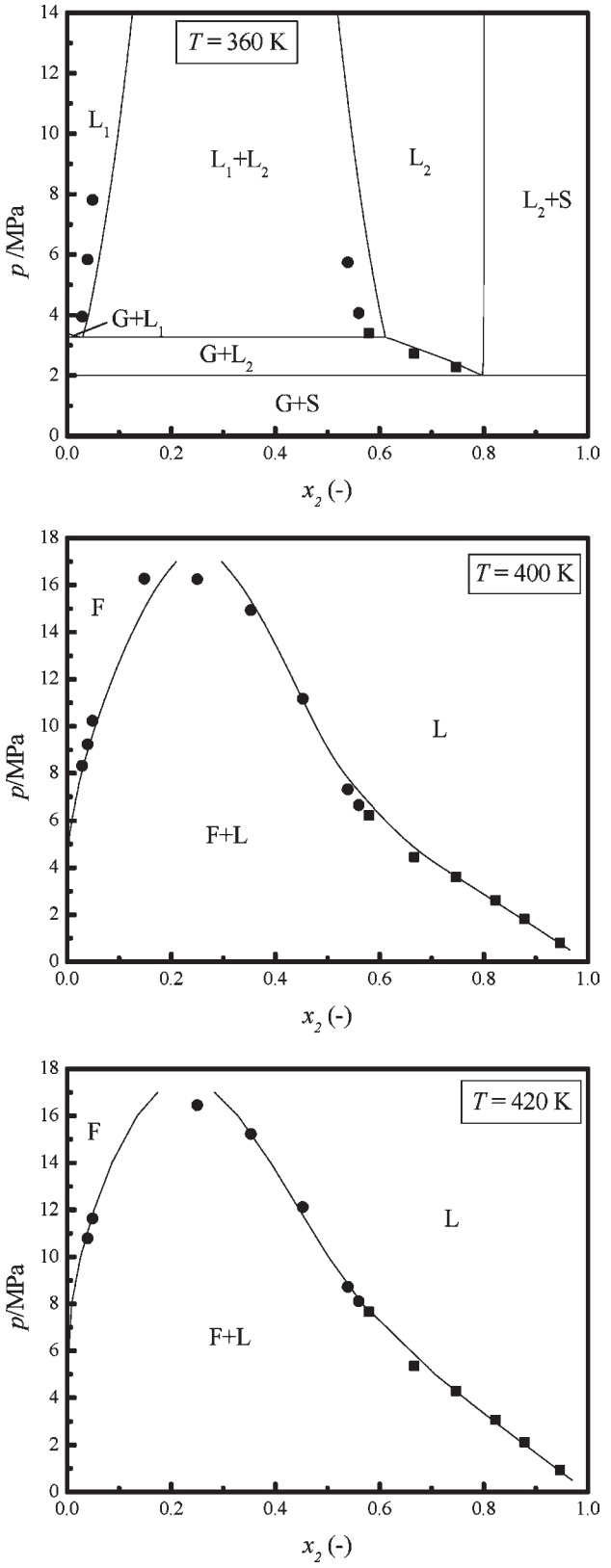

Figure 4. *p,x* diagrams for the binary system propane + phenanthrene at *T* = (360, 400, and 420) K. Comparison between predictions with the GC-EoS (lines) and experimental data (symbols). The solid circles indicate $L_1(L_2)$ or $L_2(L_1)$ experimental data and the solid cubes indicate $L_2(G)$ experimental data.

dx.doi.org/10.1021/je101058b |*J. Chem. Eng. Data* 2011, 56, 1407–1413

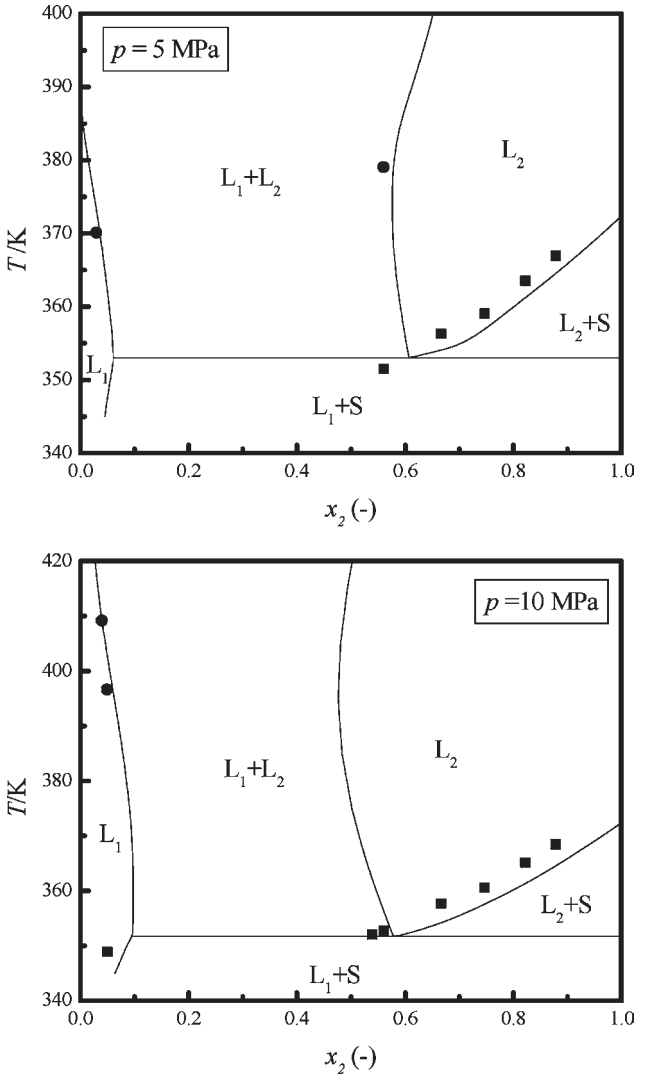

Figure 5. *T,x* diagrams for the binary system propane-phenanthrene at p = 5 MPa (top) and p = 10 MPa (bottom). Comparison between predictions with the GC-EoS (lines) and experimental data (symbols). The solid circles indicate $L_1(L_2)$ or $L_2(L_1)$ experimental data and the solid cubes indicate $L_1(S)$ or $L_2(S)$ experimental data.

place between approximately (320 and 348) K, whereas ref 16 and 17 report the temperature ranges T = (331 to 361) K and T = (331 to 344) K, respectively.

In Figure 4 *p,x* diagrams are plotted for three temperatures, namely T = (360, 400, and 420) K.

Figure 5 presents *T,x* diagrams at p = (5 and 10) MPa. In both figures a comparison is made between experimental data (symbols) and model predictions (lines). At 360 K regions can be observed with L_1G, L_2G, L_1L_2, and SL_1 two phase equilibria depending on the pressure and the overall composition of the mixture. Also two triple points can be observed (SL_2G and L_1L_2G). At (400 and 420) K only liquid-fluid equilibria are observed, because these temperatures are above the temperature of the K-point. The model predictions correspond well with the experimental data.

In both *T,x* diagrams of Figure 5 liquid−solid equilibria are observed at low temperatures. At higher temperatures both liquid−liquid equilibria and solid−liquid equilibria can be present. The GC-EoS predicts a small shift to lower temperatures for the locus of the line that separates the L_2 region from the SL_2 region.

CONCLUSIONS

Experimental data are presented on the phase behavior of binary systems of propane and phenanthrene. This system shows a complex phase behavior as a result of the presence of a solid phenanthrene phase. Bubble point lines, melting point lines and L_1L_2-miscibility lines were measured, as well as the locations of four three phase equilibria. Based on track of the latter curves the position of the quadruple point SL_1L_2G was estimated at 351.2 K and 2.928 MPa. Comparison between experimental data and model predictions on a *p,T* diagram shows that the GC-EoS predicts a shift in the position of the Q-point to slightly lower pressures and temperatures. This in turn affects the course of the three phase equilibria. Comparison of the experimental data with models predictions using *p,x* and *T,x* diagrams generally show that the complex phase behavior propane-phenanthrene systems can satisfactorily be predicted with the GC-EoS.

AUTHOR INFORMATION

Corresponding Author

*E-mail: cpeters@pi.ac.ae; C.J.Peters@tudelft.nl.

ACKNOWLEDGMENT

We would like to thank Á. Martín Martínez from the University of Valladolid for providing us with the numerical routines for the phase behavior analysis.

REFERENCES

(1) Peters, C. J. Multiphase equilibria in near-critical solvents. In *Supercritical Fluid Fundamentals for Application* Kiran, E., Levelt-Sengers., J. M. H., Eds.; Series E: Applied Sciences. 1994, 273, 117-145.

(2) Peters, C. J.; De Roo, J. L.; De Swaan Arons, J. Phase equilibria in binary mixtures of propane and triphenylmethane. *Fluid Phase Equilib.* **1995**, *109*, 99–111.

(3) Van Konynenburg, P. N.; Scott, R. L. Critical lines and phase equilibria in binary van der Waals mixtures. *Phil. Trans. R. Soc.* **1980**, *298*, 495–540.

(4) De Loos, Th.W.; Van der Kooi, H. J.; Poot, W.; Ott, P. L. Fluid phase equilibria in the system ethylene-vinyl chloride. *Delft Prog. Rep. Ser. A* **1983**, *8*, 200.

(5) Peters, C. J.; De Roo, J. L.; De Swaan Arons, J. Phase equlibria in binary mixtures of propane and hexacontane. *Fluid Phase Equilib.* **1993**, *85*, 301–312.

(6) Kühne, E.; Santarossa, S.; Witkamp, G. J.; Peters, C. J. Phase equilibria in ternary mixtures of the ionic liquid bmim[BF_4], (*S*)-naproxen and CO_2 to determine optimum regions for green processing. *Green Chem.* **2008**, *10*, 762–766.

(7) Skjold-Jørgensen, S. Gas solubility calculations. II. Application of a new group-contribution equation of state. *Fluid Phase Equilib.* **1984**, *16*, 317–351.

(8) Skjold-Jørgensen, S. Group Contribution Equation of State (GC-EOS): a Predictive Method for Phase Equilibrium Computations over Wide Ranges of Temperatures and Pressures up to 30 MPa. *Ind. Eng. Chem. Res.* **1988**, *27*, 110–118.

(9) Fornari, T. Revision and summary of the group contribution equation of state parameter table: Application to edible oil constituents. *Fluid Phase Equilib.* **2007**, *262*, 187–209.

(10) Poling, B. E.; Prausnitz, J. M.; O'Connell, J. P. *The properties of gases and liquids*; 5th Ed.; McGraw-Hill: London, 2001.

(11) Hodgman, C. D.; Weast, R. C.; Lide, D. R. *CRC Handbook of Chemistry and Physics*; CRC Press: Boca Raton, 2001/2002.
(12) Mortimer, F. S.; Murphy, R. V. The vapor pressures of some substances found in coal tar. *Ind. Eng. Chem.* **1923**, *15*, 1140–1142.
(13) Choi, P. B.; McLaughlin, E. Effect of a phase transition on the solubility of a solid. *AIChE J.* **1983**, *29*, 150–153.
(14) Finke, H. L.; Messerly, J. F.; Lee, S. H.; Osborn, A. G.; Diuslin, D. R. Comprehensive thermodynamic studies of seven aromatic hydrocarbons. *J. Chem. Thermodyn.* **1977**, *9*, 937–956.
(15) Gupta, A. K.; Bishnoi, P. R.; Kalogerakis, N. A method for the simultaneous phase equilibria and stability calculations for multiphase reacting and non-reacting systems. *Fluid Phase Equilib.* **1991**, *63*, 65–89.
(16) Arndt, R. A.; Damask, A. C. Heat capacity anomaly in phenanthrene. *J. Chem. Phys.* **1966**, *45*, 755–756.
(17) Casellato, F.; Vecchi, C.; Girelli, A. Differential calorimetric study of polycyclic aromatic hydrocarbons. *Thermochim. Acta* **1973**, *6*, 361–368.